Revisiting and Optimizing the Design of the Timer-Based Distributed Selection Scheme for Tackling Imperfect Power Control

Vikas Kumar Dewangan and Neelesh B. Mehta, *Senior Member, IEEE*

***Abstract*— Opportunistic selection improves the performance of a multi-node wireless system by exploiting multi-user or spatial diversity. In it, the nodes are sorted in the descending order of their metrics, which captures the utility of a node to the system if selected, and the best node with the highest metric is selected. We analyze the effect of imperfect power control on the conventional timer with power control scheme, which selects the best node in a distributed manner, and quantify the extent by which it reduces the probability of selecting the best node and increases the probability of selecting a non-best node. We then redesign it to ameliorate the impact of imperfect power control. Our systematic approach eschews several *ad hoc* assumptions implicit in the design of the conventional timer scheme, and jointly optimizes its various parameters to maximize the probability of selecting the best node in the presence of imperfect power control. We present several structural insights, including asymptotic ones, about the optimal scheme, which also enable it to be determined with much lower computational complexity. Our benchmarking results show that it is scalable and outperforms the conventional schemes.**

***Index Terms*— Selection, capture, power control, medium access control, timer.**

I. Introduction

OPPORTUNISTIC selection improves the performance of many multi-node wireless systems by selecting one node among the available nodes for data transmission. For example, in a cooperative relaying system, selecting the relay that maximizes the signal-to-noise ratio (SNR) at the destination to forward the source's message to the destination achieves the same diversity order as having all the relays forward the message simultaneously, while avoiding the tight synchronization requirement among the relays [1], [2]. In cellular systems, selecting the mobile with the highest downlink channel power gain increases the spectral efficiency and throughput [3, Ch. 14]. In wireless sensor networks, selecting the sensor node based on its battery energy increases network lifetime and reduces energy consumption [4].

Manuscript received April 5, 2017; revised July 5, 2017; accepted September 5, 2017. Date of publication September 19, 2017; date of current version November 9, 2017. This work was supported in part by the DST-Swaranajayanti Fellowship Award under Grant DST/SJF/ETA-01/2014-15. The associate editor coordinating the review of this paper and approving it for publication was A. Banchs. *(Corresponding author: Neelesh B. Mehta.)*

V. K. Dewangan is with the Electronics and Radar Development Establishment, Bengaluru, India (e-mail: dewangan.vikaskumar@gmail.com).

N. B. Mehta is with the Department of Electrical Communication Engineering, Indian Institute of Science, Bengaluru, India (e-mail: neeleshbmehta@gmail.com).

Digital Object Identifier 10.1109/TWC.2017.2752157

Opportunistic selection can be formally defined as follows. Each node possesses a real-valued metric, which is application-dependent and measures its ability to improve the system performance if selected. In the cooperative relaying system example above, a relay's metric is its end-to-end SNR. In the cellular system example above, a mobile's metric is its downlink channel power gain. We note that even user fairness can be incorporated into this framework by suitably defining the metric [5]. *The best node, which is the node that needs to be selected, is defined as the node with the largest metric.*

While opportunistic selection is appealing, identifying the best node is a practical challenge because a node only knows its metric. Therefore, no node in the network initially knows who the best node is. Consequently, a selection scheme is required to identify the best node. For example, in the centralized polling scheme [6], [7], each node sequentially conveys its metric to a coordinating node, which can then identify the best node. However, its drawback is that the time taken to convey the metrics of all the nodes grows linearly in the number of nodes. This overhead degrades the overall system performance and makes it sensitive to time variations in the channel. Therefore, distributed and scalable selection schemes are necessary. The timer scheme is one such widely used scheme [6]–[10], and is the focus of this paper.

A. Timer Scheme Overview

In it, a node j sets its timer as a function of its metric μ_j, and transmits its packet to a coordinating node called sink when its timer expires [8], [9]. The metric-to-timer mapping is monotone non-increasing, which ensures that the best node always transmits first. In a practical system, the timer packets have a non-zero duration. Hence, if the best node's transmission overlaps with another node's transmission, which happens if their timers expire within a time interval Δ_v [6], [7], [10], then a collision is said to occur and the scheme fails to select the best node. This model has been extensively used in the multiple access literature [6], [8], [11]–[14], and Δ_v is often referred to as the vulnerability window. If the nodes employ carrier sense multiple access with collision avoidance (CSMA/CA), then Δ_v is determined by propagation delays and time synchronization errors between the nodes, and switching times, as explained in detail in [7] and [8]. When the nodes lack the CSMA/CA capability, then Δ_v also accounts for the packet duration and, hence, is larger.

While the timer scheme is simple, we saw that it can fail to select the best node for some realizations of the metrics. Hence, *the probability that the best node gets selected, which we shall henceforth refer to as the success probability*, is an important performance measure for it. The following techniques have been employed to improve it.

- *Optimization of Metric-to-Timer Mapping:* For a selection duration $T_{\max}$, which the system allocates for selection, an optimal mapping is derived in [6] that maps the metrics into discrete timer values, namely $0, \Delta_v, \ldots, N\Delta_v$, where $N = \lfloor T_{\max}/\Delta_v \rfloor$ and $\lfloor \cdot \rfloor$ denotes the floor function. Furthermore, it is characterized in a recursive manner. We shall refer to this as the conventional timer (CT) scheme. It is shown in [6] that the CT scheme markedly outperforms the popular inverse timer (IT) scheme [8].
- *Power Control:* In the conventional timer with power control (CTPC) scheme, a node not only sets its timer based on its metric but also controls its transmit power to achieve a pre-specified target receive power level at the sink [14]. The target receive power levels are designed to exploit the capture effect, as per which a node gets selected even if other nodes interfere with it as long as its SNR or signal-to-interference-plus-noise-ratio (SINR) exceeds a decoding threshold γ [15], [16], [17, Ch. 8].[1] This SINR-based decoding model is more realistic than the conventional collision model that has been used in most papers on timer-based selection [6]–[8]. The latter assumes that when one node transmits, a success inevitably occurs, and when the transmissions of two or more nodes overlap in time, then a collision inevitably occurs.

However, several open questions remain about the efficacy of power control in practical systems, especially when it is imperfect. Imperfect power control affects the timer scheme's performance because it can cause a node's receive power to deviate from its target. Consequently, the receiver can fail to decode the packet from the best node if its receive signal strength decreases or the interference from other nodes increases sufficiently.

B. Contributions, Connections, and Differences from Related Works

In this paper, we first analyze the impact of imperfect power control on the CTPC scheme [14]. We focus on the CTPC scheme as it achieves the highest success probability among all the known timer schemes and it does so by exploiting power control. We then develop a formal methodology to optimize the timer scheme's performance in the presence of imperfect power control that eschews several assumptions implicitly made by the CTPC scheme. While the impact of imperfect power control on many wireless systems, which includes multiple access control (MAC) protocols and the splitting-based selection scheme, has been well studied, its impact on the timer scheme has not been characterized to the best of our knowledge [18]–[21].

1) Analysis of CTPC Scheme: We first characterize and quantify the effect of imperfect power control on the CTPC scheme. For this, we employ a theoretically and practically well-motivated lognormal power control error model that captures the combined effect of imperfect channel estimation and a multitude of non-idealities at the transmitter and receiver. We show that imperfect power control reduces the scheme's success probability. It also causes the probability of selecting a non-best node, which is zero under perfect power control, to become non-zero.

2) Optimization of Timer Scheme: Our second contribution is the design of an optimal imperfect power control-aware timer scheme. For this, we optimize the metric-to-timer-and-power mapping to maximize the success probability under imperfect power control. We focus on the two target receive power levels scenario because it is tractable and insightful, and since increasing the number of power levels further yields marginal gains [14]. We also optimize the lower target receive power level as a function of the timer value. This is unlike the CTPC scheme, in which it is an ad hoc constant that needs to be pre-specified. In order to enable a fair comparison across schemes and to capture the hardware constraints imposed by the dynamic range of power levels that the receiver circuitry can handle, this design is done given a high target receive power level H.

Our formal approach explores the following trade-off that arises between the success probability and the lower target receive power level L. When the best node transmits alone and targets a receive power level L, the success probability increases as L increases since it improves the odds that the resultant SNR exceeds γ. On the other hand, when the best node transmits and targets the receive power level H, and other nodes transmit simultaneously and target the receive power level L, the success probability decreases as L increases since the interference power is proportional to L. Controlling this interference is one of the key issues that drives the design of the optimal scheme.

As we shall see, the optimization is more challenging than for CTPC because the number of variables is larger and since the physical layer model is more sophisticated. We show that the optimal parameters can be efficiently computed in a recursive manner. Finally, we show that its success probability is higher than several other timer schemes.

3) Asymptotic Analysis: To gain significant insights, we analyze the asymptotic regime of a large number of nodes. We derive an insightful perturbation-theoretic result that explicitly reveals how the statistics of imperfect power control affect the optimal parameters.

C. Organization

The paper is organized as follows. Section II presents the system model. The impact of imperfect power control on the CTPC scheme is analyzed in Section III. In Section IV, we optimize the timer scheme to tackle imperfect power control and analyze its performance. Numerical results are

[1] The threshold γ depends on the modulation and coding scheme, and is of the order of 8 to 10 dB. Code division multiple access systems require lower decoding thresholds, but at the expense of extra bandwidth. We do not consider these systems in this paper. Thus, in our model at most one node can get selected.

presented in the Section V, and are followed by our conclusions in Section VI.

II. Preliminaries and System Model

We shall use the following notation. The probability of an event $\mathcal{E}$ is denoted by $\Pr\{\mathcal{E}\}$. The conditional probability of $\mathcal{E}$ given $\mathcal{F}$ is denoted by $\Pr\{\mathcal{E}|\mathcal{F}\}$. A Gaussian random variable (RV) X with mean μ and variance σ^2 is denoted by $X \sim \mathcal{N}(\mu, \sigma^2)$. For a lognormal RV Z, the mean and standard deviation of $\ln(Z)$, which is a Gaussian RV, shall be referred to as the log-mean and the log-deviation, respectively, of Z. The multinomial term $\binom{K}{j_1, j_2, \ldots, j_n}$ stands for $K!/\left(j_1!j_2!\ldots j_n!(K - j_1 - j_2 - \ldots - j_n)!\right)$.

Consider a multi-node system with $K \geq 2$ nodes. Each node j has a real-valued metric μ_j, which only it knows. The metrics are assumed to be independent and identically distributed (i.i.d.) RVs [6], [14], [22]. The independence assumption is justified, for example, when the metrics depend on the channel gains and the nodes are spaced many wavelengths apart. The assumption about statistically identical metrics makes the optimization problem tractable, and is also made in [6], [7], [14], and [22]–[24]. Let μ_j have a continuous cumulative distribution function (CDF) $C(\cdot)$. Then, consider the following new metric $\kappa_j = C(\mu_j)$ for node j. It is uniformly distributed between $[0, 1)$ and preserves order [25]. We, therefore, assume without loss of generality (w.l.o.g.) that the metric is uniformly distributed in $[0, 1)$. Since the CDF changes at a rate that is several orders of magnitude slower than the metrics, it can be estimated accurately with minimal signaling overhead [26].

Following order statistics notation, let $[j]$ denote the node with the j^{th} largest metric $\mu_{[j]}$. Therefore, $\mu_{[1]} \geq \mu_{[2]} \geq \cdots \geq \mu_{[K]}$. Here, [1] is the best node and $[2], \ldots, [K]$ are non-best nodes. During the selection process, which lasts for a duration $T_{\max}$, the sink receives the transmissions of the nodes. The nodes transmit on the same MAC channel and, therefore, interfere with each other if their timers expire within the time interval Δ_v of each other. The target receive power level of node $[j]$ is denoted by $q_{[j]}$.

A. Background: CTPC

We first summarize below the CTPC scheme, which was proposed in [13], to set up key notation and to enumerate the key concepts behind combining power control with the timer scheme. For a given selection duration $T_{\max}$, every node transmits only at discrete time instants $0, \Delta_v, \ldots, N\Delta_v$, where $N = \lfloor T_{\max}/\Delta_v \rfloor$.[2] Given the equivalence between N and $T_{\max}$, we shall henceforth refer to N also as the selection duration. The scheme is characterized by an interval length vector (ILV) $\boldsymbol{\alpha}_N = [\alpha_N[0], \alpha_N[1], \ldots, \alpha_N[N]]$, which determines when a node transmits, and a power distribution vector (PDV) $\boldsymbol{f}_N = [f_N[0], f_N[1], \ldots, f_N[N]]$, which determines its target

[2]In practice, the nodes need not be perfectly synchronized. As discussed in Section I-A, the synchronization error and propagation delays are captured in Δ_v.

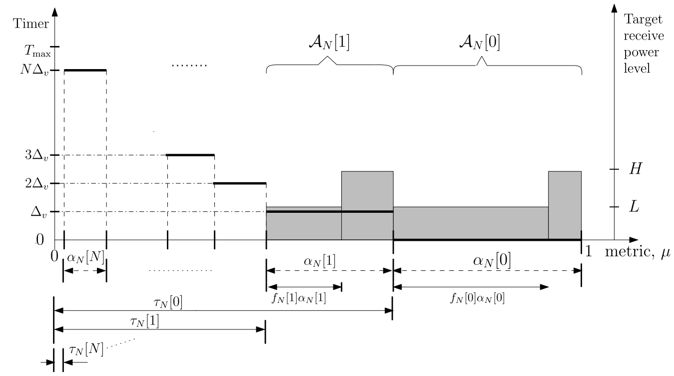

Fig. 1. Illustration of the metric-to-timer-and-power mapping of the CTPC scheme and how different metrics lead to different timers and target receive power levels. The shaded vertical bars represent target receive power levels.

receive power level when it transmits. Specifically, as illustrated in Fig. 1, a node transmits at time $t = i\Delta_v$ if its metric lies in the interval

$$\mathcal{A}_N[i] \triangleq [\tau_N[i], \tau_N[i] + \alpha_N[i]), \tag{1}$$

where $\tau_N[i] = 1 - \sum_{l=0}^{i} \alpha_N[l]$, for $0 \leq i \leq N$, $\alpha_N[l] \geq 0$, and $\sum_{l=0}^{N} \alpha_N[l] \leq 1$. It means that nodes whose metrics lie in $[1 - \alpha_N[0], 1)$ transmit at time 0, nodes whose metrics lie in $[1 - \alpha_N[0] - \alpha_N[1], 1 - \alpha_N[0])$ transmit at time Δ_v, and so on. Nodes whose metrics lie in $[0, 1 - \sum_{i=0}^{N} \alpha_N[i])$ do not transmit. We shall refer to i as the interval index. Since the metric-to-timer mapping here is monotonically non-increasing, the best node always transmits first.

Furthermore, as shown in Fig. 1, the interval $\mathcal{A}_N[i]$ is subdivided into two sub-intervals. A node that transmits at time $i\Delta_v$ sets its target receive power level as L if its metric lies in $[\tau_N[i], \tau_N[i] + \alpha_N[i] f_N[i])$, and as H otherwise. Clearly, $0 \leq f_N[i] \leq 1$, for $0 \leq i \leq N$. The scheme is specified in terms of the target receive power levels because it is the receive power level of the transmitting node(s) that ultimately determines their SNR or SINR. It is also for this reason that classical power control schemes are designed for a target receive power level [3, Ch. 13]. The target receive power levels are specified in [14] as

$$L = \gamma\sigma^2 \quad \text{and} \quad H = \gamma(\eta L + \sigma^2), \tag{2}$$

where σ^2 is the noise power. This setting of H ensures that the best node is decoded if it transmits and has receive power level H and even if up to η other nodes transmit simultaneously and each of them has receive power level L. And, L is set so that the best node gets decoded if it transmits alone and its receive power level is L. The parameter η is known as the *adversary order*. Equations (1) and (2) ensure that the best node transmits no later than any other node and that it targets a receive power level that is no less than that of any other node that transmits simultaneously with it. Hence, the scheme guarantees that a node, if selected, is the best node. As $(\boldsymbol{\alpha}_N, \boldsymbol{f}_N)$ specifies the mapping, we will henceforth use the tuple $(\boldsymbol{\alpha}_N, \boldsymbol{f}_N)$ to refer to the scheme itself.

1) Transmit Power Setting: In order to achieve a target receive power level $q_{[j]}$, node $[j]$ sets its transmit power $P_{[j]}^{\text{tx}}$

as $q_{[j]}/h_{[j]}$, where $h_{[j]}$ is the channel power gain from the node to the sink. Consequently, the signal power $P_{[j]}^{\text{rx}}$ at the receiver is equal to

$$P_{[j]}^{\text{rx}} = h_{[j]} P_{[j]}^{\text{tx}} = h_{[j]} \frac{q_{[j]}}{h_{[j]}} = q_{[j]}. \tag{3}$$

In time division duplexing (TDD), a node can know its channel power gain by exploiting reciprocity; no feedback is required. In frequency division duplexing (FDD), periodic feedback from the sink is required.

2) Optimal Parameters: The optimal $\boldsymbol{\alpha}_N$ and $\boldsymbol{f}_N$ that maximize the success probability of the CTPC scheme depend on η; they are not known in general. However, in [14], the optimal solution is given in a recursive form for $\eta = 1$, and a solution that maximizes a lower bound on the success probability is given for $\eta = 2$.

B. Imperfect Power Control: Model and Implications

In practice, due to an inaccurate estimate of the channel power gain, imperfect RF chain calibration in case of TDD, feedback errors and delays in case of FDD, and non-idealities at the transmitter such as quantization effects, power control algorithm used, rate of adaptation of power, and dynamic range of the transmitter [18], the transmit power of node $[j]$ ends up getting set as $P_{[j]}^{\text{tx}} = \left(q_{[j]}/\widehat{h}_{[j]}\right) \varepsilon_{[j]}^{\text{tx}}$, where $\widehat{h}_{[j]}$ is the estimate of $h_{[j]}$ available at node $[j]$ and $\varepsilon_{[j]}^{\text{tx}}$ is the net contribution of the non-idealities at the transmitter of node $[j]$. Hence, the received signal power $P_{[j]}^{\text{rx}}$ of node $[j]$ is equal to

$$P_{[j]}^{\text{rx}} = h_{[j]} P_{[j]}^{\text{tx}} \varepsilon_{[j]}^{\text{rx}} = q_{[j]} \frac{h_{[j]}}{\widehat{h}_{[j]}} \varepsilon_{[j]}^{\text{tx}} \varepsilon_{[j]}^{\text{rx}}, \tag{4}$$

where $\varepsilon_{[j]}^{\text{rx}}$ is the net contribution of the non-idealities at the receiver due to quantization, receiver-side filtering, etc. [27]. The factor $\left(h_{[j]}/\widehat{h}_{[j]}\right) \varepsilon_{[j]}^{\text{tx}} \varepsilon_{[j]}^{\text{rx}}$ is defined as the *power control error*. Extensive experimental measurement campaigns and theoretical investigations show that the power control error is well modeled as a lognormal RV [27]–[31]. Hence, $P_{[j]}^{\text{rx}}$ can be written as

$$P_{[j]}^{\text{rx}} = q_{[j]} e^{l_{[j]}}, \tag{5}$$

where $l_{[j]} \sim \mathcal{N}(0, \sigma_l^2)$. Typically, σ_l is of the order of 0.23 to 0.46.[3] Henceforth, when we say that node $[j]$ targets a receive power level $q_{[j]}$ at time $i\Delta_\upsilon$, we mean that it transmits with power $\left(q_{[j]}/\widehat{h}_{[j]}\right) \varepsilon_{[j]}^{\text{tx}}$ at time $i\Delta_\upsilon$ and, consequently, its receive power is equal to $q_{[j]} e^{l_{[j]}}$.

When the best node transmits alone, its SNR is equal to $q_{[1]} e^{l_{[1]}}/\sigma^2$. And, in general, when the M nodes $[1], [2], \ldots, [M]$ transmit simultaneously and target the receive power levels $q_{[1]}, \ldots, q_{[M]}$, respectively, the SINR of node $[j]$, which is denoted by $\text{SINR}_{[j]}$, equals

$$\text{SINR}_{[j]} = \frac{q_{[j]} e^{l_{[j]}}}{\sum_{k=1, k\neq j}^{M} q_{[k]} e^{l_{[k]}} + \sigma^2}, \quad \text{for } 1 \le j \le M. \tag{6}$$

[3]In the lognormal literature, dB units are typically used. For a log-deviation of σ_l, the standard deviation in dB is equal to $10\sigma_l/\ln(10)$. It is reported as being of the order of 1-2 dB [18], [30], which corresponds to the values mentioned above.

The best node gets selected only if $\text{SINR}_{[1]}$ exceeds γ. Since $q_{[1]} \ge q_{[2]} \ge \cdots \ge q_{[M]}$, it follows for perfect power control ($\sigma_l = 0$) that $\text{SINR}_{[j]} < 1 < \gamma$, for $2 \le j \le M$. Thus, a non-best node never gets selected with perfect power control. However, imperfect power control can cause $\text{SINR}_{[j]}$ to exceed γ, for some non-best node and lead to its selection.

III. Analysis of Impact of Imperfect Power Control

We now analyze the impact of imperfect power control on the CTPC scheme. To do so, we define $\mathcal{S}_{m,n}(i)$ as the event that nodes $[1], \ldots, [n]$ target the receive power level H and nodes $[n+1], \ldots, [n+m]$ target the receive power level L at time $i\Delta_\upsilon$. Further, in order to make analysis tractable, we make the following two intuitive approximations and illustrate their accuracy with an example in which $K = 10$, $\eta = 1$, $N = 14$, $\gamma = 10$, $\sigma = 1$, and $\sigma_l = 1$. They are as follows: (i) The probability that four or more nodes transmit simultaneously is negligible. For the above example, it turns out to be just 0.005. (ii) If three nodes target the same receive power level simultaneously, then the probability that any of them gets selected can be neglected. For the above example, this probability is just 0.0015.

The following two results characterize the impact of imperfect power control on the CTPC scheme.

Result 1: The success probability P_N of the CTPC scheme in the presence of imperfect power control is given by

$$P_N = \sum_{i=0}^{N} \sum_{m=0}^{K} \sum_{n=0}^{K-m} \varpi_{m,n} \binom{K}{m,n} (\tau_N[i])^{K-(m+n)} \times (\alpha_N[i])^{m+n} (f_N[i])^m (1 - f_N[i])^n, \tag{7}$$

where $\varpi_{(m,n)}$ is the probability of success given the event $\mathcal{S}_{m,n}(i)$ and is given by

$$\varpi_{m,n} = \begin{cases} 0, & m = 0, n = 0, \\ Q\left(\frac{1}{\sigma_l} \ln\left(\frac{\gamma\sigma^2}{\tilde{q}}\right)\right), & m + n = 1, \\ Q\left(\frac{\ln(\gamma/\tilde{q}) + \mu'_{m,n}}{\sqrt{\sigma_l^2 + \sigma'^2_{m,n}}}\right), & \text{otherwise.} \end{cases} \tag{8}$$

Here, $Q(x)$ is the Gaussian Q-function, and $\tilde{q} = H$, if $n \ge 1$, and $\tilde{q} = L$, if $n = 0$. Furthermore,

$$\sigma'^2_{m,n} = \begin{cases} \ln\left(\frac{g(n-1,m)}{(h(n-1,m))^2} + 1\right), & n \ge 1, \\ \ln\left(\frac{g(0,m-1)}{(h(0,m-1))^2} + 1\right), & \text{otherwise,} \end{cases} \tag{9}$$

$$\mu'_{m,n} = \begin{cases} \ln(h(n-1,m)) - \frac{\sigma'^2_{m,n}}{2}, & n \ge 1, \\ \ln(h(0,m-1)) - \frac{\sigma'^2_{m,n}}{2}, & \text{otherwise,} \end{cases} \tag{10}$$

$g(n,m) = e^{\sigma_l^2}\left(e^{\sigma_l^2} - 1\right)\left(nH^2 + mL^2\right)$, and $h(n,m) = e^{\sigma_l^2/2}(nH + mL) + \sigma^2$.

Proof: The proof is relegated to Appendix A.

Explanation: In (7), the term $\binom{K}{m,n}(\tau_N[i])^{K-(m+n)}$ $(\alpha_N[i])^{m+n}(f_N[i])^m(1-f_N[i])^n$ is the probability of $\mathcal{S}_{m,n}(i)$. And, in (8), $\mu'_{m,n}$ and $\sigma'_{m,n}$ are the log-mean and log-deviation, respectively, of the interference plus noise power while decoding the transmission of the best node given the event $\mathcal{S}_{m,n}(i)$. ■

Result 2: The probability P_N^{other} that a non-best node gets selected is

$$P_N^{\text{other}} = \sum_{i=0}^{N}\sum_{m=0}^{K}\sum_{n=0}^{K-m}\varpi'_{m,n}\binom{K}{m,n}(\tau_N[i])^{K-(m+n)} \times (\alpha_N[i])^{m+n}(f_N[i])^m(1-f_N[i])^n, \quad (11)$$

where $\varpi'_{(m,n)}$ is the probability that a non-best node gets selected given the event $\mathcal{S}_{m,n}(i)$ and is given by

$$\varpi'_{m,n} = \begin{cases} 0, & m+n \le 1, \\ Q\left(\dfrac{\ln(\gamma/\tilde{q}) + \mu''_{m,n}}{\sqrt{\sigma_l^2 + \sigma''^2_{m,n}}}\right), & \text{otherwise.} \end{cases} \quad (12)$$

Here, $\tilde{q}$ is H, if $n \ge 2$, and is L, otherwise. Furthermore,

$$\sigma''^2_{m,n} = \begin{cases} \ln\left(\dfrac{g(1,m-1)}{(h(1,m-1))^2}+1\right), & n=1, \\ \ln\left(\dfrac{g(n-1,m)}{(h(n-1,m))^2}+1\right), & n \ge 2, \\ \ln\left(\dfrac{g(0,m-1)}{(h(0,m-1))^2}+1\right), & \text{otherwise,} \end{cases} \quad (13)$$

$$\mu''_{m,n} = \begin{cases} \ln(h(1,m-1)) - \dfrac{\sigma''^2_{m,n}}{2}, & n=1, \\ \ln(h(n-1,m)) - \dfrac{\sigma''^2_{m,n}}{2}, & n \ge 2, \\ \ln(h(0,m-1)) - \dfrac{\sigma''^2_{m,n}}{2}, & \text{otherwise.} \end{cases} \quad (14)$$

Proof: The proof is relegated to Appendix B. ■

In (12), $\mu''_{m,n}$ and $\sigma''_{m,n}$ are the log-mean and log-deviation, respectively, of the interference plus noise power while decoding the transmission of the non-best node given $\mathcal{S}_{m,n}(i)$.

IV. Optimal Timer Scheme for Imperfect Power Control

We now redesign the timer scheme to maximize its success probability for imperfect power control for a given selection duration $N \in \mathbb{Z}^+$, and for a given $H > 0$. Instead of pre-specifying parameters such as η and L in an ad hoc manner, we jointly optimize $\boldsymbol{\alpha}_N$, $\boldsymbol{f}_N$, and the lower target receive power level $L_N[i] \le H$ for each interval index i. Thus, a node that transmits at $i\Delta_\upsilon$ targets a receive power level that belongs to the set $\{L_N[i], H\}$. Let the *lower power* vector (LPV) $\boldsymbol{L}_N$ be defined as

$$\boldsymbol{L}_N \triangleq [L_N[0], L_N[1], \ldots, L_N[N]]. \quad (15)$$

We shall use the triplet $(\boldsymbol{\alpha}_N, \boldsymbol{f}_N, \boldsymbol{L}_N)$ to refer to the scheme itself, and shall denote its success probability by $P_N(\boldsymbol{\alpha}_N, \boldsymbol{f}_N, \boldsymbol{L}_N)$. The total number of variables to be optimized jointly is $3(N+1)$. Let P_N^* denote the optimal success probability, and let $\boldsymbol{\alpha}_N^*$, $\boldsymbol{f}_N^*$, and $\boldsymbol{L}_N^*$ denote the optimal ILV, PDV, and LPV, respectively, that achieve it. We now derive a general recursion that governs the optimal parameters and the optimal success probability for imperfect power control.

General Recursion: From the law of total probability, $P_N(\boldsymbol{\alpha}_N, \boldsymbol{f}_N, \boldsymbol{L}_N)$ is given by

$$\begin{aligned} &P_N(\boldsymbol{\alpha}_N, \boldsymbol{f}_N, \boldsymbol{L}_N) \\ &\quad = \Pr\{S_0(\alpha_N[0], f_N[0], L_N[0])\} + (1-\alpha_N[0])^K \\ &\qquad \times P_{N-1}(\boldsymbol{\alpha}'_{N-1}, \boldsymbol{f}'_{N-1}, \boldsymbol{L}'_{N-1}), \end{aligned} \quad (16)$$

where $S_0(x,y,z)$ is the success event at time 0 when $\alpha_N[0] = x$, $f_N[0] = y$, and $L_N[0] = z$ and $(1-\alpha_N[0])^K P_{N-1}(\boldsymbol{\alpha}'_{N-1}, \boldsymbol{f}'_{N-1}, \boldsymbol{L}'_{N-1})$ is the probability that a success occurs later.

Equation (16) follows because a success at a later time instant can occur only if no node transmits at time $t = 0$, for which no node's metric must lie in the interval $[1-\alpha_N[0], 1)$. This happens with probability $(1-\alpha_N[0])^K$. Given this event, the metrics of the K nodes are i.i.d. and uniformly distributed in $[0, 1-\alpha_N[0])$, and the total time available for the selection process decreases to $T_{\max} - \Delta_\upsilon$, for which the success probability is, by definition, $P_{N-1}(\boldsymbol{\alpha}'_{N-1}, \boldsymbol{f}'_{N-1}, \boldsymbol{L}'_{N-1})$. Here, the elements of the N-length vectors $\boldsymbol{\alpha}'_{N-1}$, $\boldsymbol{f}'_{N-1}$, and $\boldsymbol{L}'_{N-1}$ are given as follows, for $0 \le i \le N-1$:

$$\alpha'_{N-1}[i] = \frac{\alpha_N[i+1]}{1-\alpha_N[0]}, \quad (17a)$$

$$f'_{N-1}[i] = f_N[i+1], \quad (17b)$$

$$L'_{N-1}[i] = L_N[i+1]. \quad (17c)$$

As shown in Appendix C, $\Pr\{S_0(x,y,z)\}$ is given by

$$\begin{aligned} &\Pr\{S_0(x,y,z)\} \\ &\quad = Kx(1-x)^{K-1}(y\epsilon_1(z) + (1-y)\epsilon_1(H)) \\ &\qquad + \binom{K}{1,1}(1-x)^{K-2}x^2(1-y)y\epsilon_2(z). \end{aligned} \quad (18)$$

Here, $\epsilon_1(z) = Q\left(\ln\left(\sigma^2\gamma/z\right)/\sigma_l\right)$ is the success probability given that only node [1] transmits and its target receive power level is $q_{[1]} = z$. And, $\epsilon_2(z)$ is the success probability given that only nodes [1] and [2] transmit, and $q_{[1]} = H$ and $q_{[2]} = z$. It is equal to $Q\left(\left(\ln(\gamma/H) + \grave{\mu}\right)/\grave{\sigma}\right)$, where $\grave{\sigma}^2 = \ln\left(z^2 e^{\sigma_l^2}\left(e^{\sigma_l^2}-1\right)/\left(ze^{\sigma_l^2/2}+\sigma^2\right)^2 + 1\right)$ and $\grave{\mu} = \ln\left(ze^{\sigma_l^2/2}+\sigma^2\right) - \grave{\sigma}^2/2$.

Equation (16) implies the following recursion that involves just three variables:

$$\begin{aligned} &\left(\alpha_N^*[0], f_N^*[0], L_N^*[0]\right) \\ &\quad = \operatorname*{argmax}_{0\le x,y\le 1,\, 0\le z\le H}\left\{\Pr\{S_0(x,y,z)\} + (1-x)^K P_{N-1}^*\right\}, \end{aligned} \quad (19)$$

and the optimal success probability is given by

$$P_N^* = \Pr\left\{S_0(\alpha_N^*[0], f_N^*[0], L_N^*[0])\right\} + (1-\alpha_N^*[0])^K P_{N-1}^*, \tag{20}$$

with $P_{-1}^* \triangleq 0$. This recursion is similar to that for the CTPC scheme with perfect power control [14, (11)] though the models are different.

Result 3: The following statements show that only one variable $L_N[0]$ needs to be numerically optimized, while the other two optimal parameters can be deduced from it:

1) Given $\alpha_N[0] = x$ and $L_N[0] = z$, the fraction $f_N[0]$ that maximizes the success probability is equal to $1/2 - (1-x)\,(\epsilon_1(H) - \epsilon_1(z))\,/\,(2(K-1)x\epsilon_2(z))$.
2) Given $L_N[0] = z$, the interval length $\alpha_N[0]$ that maximizes the success probability is a solution of the following quadratic equation:

$$a(z)x^2 + b(z)x + c = 0, \tag{21}$$

where

$$a(z) = K\left(\chi_1(z) - \frac{\chi_2(z)}{2} - \frac{\chi_3(z)}{2}\right) - P_{N-1}^*,$$
$$b(z) = \chi_2(z) + K\chi_3(z) - (K+1)\chi_1(z) + 2P_{N-1}^*,$$
$$c(z) = \chi_1(z) - \frac{K\chi_3(z)}{2} - P_{N-1}^*,$$

$\chi_1(z) = (\epsilon_1(z) + \epsilon_1(H))/2$, $\chi_2(z) = (K-1)\,\epsilon_2(z)/2$, and $\chi_3(z) = (\epsilon_1(z) - \epsilon_1(H))^2/(2(K-1)\epsilon_2(z))$.

Proof: The proof is given in Appendix D. ■

Comments:

- By the virtue of (19) and Result 3, the total number of variables that need to be jointly optimized numerically decreases from $3(N+1)$ to 1. The only variable that needs to be optimized numerically is $L_N[0]$, which is determined in terms of the parameters optimized for $N-1$. The optimal parameters need to be obtained only once at the beginning of the selection process, and can be conveyed to all the nodes.
- Under perfect power control, if $L_N^*[0] \geq \gamma\sigma^2$ and $H = \gamma(L_N^*[0] + \sigma^2)$, then $\epsilon_1(L_N^*[0]) = \epsilon_1(H) = \epsilon_2(L_N^*[0]) = 1$. Substituting these values in Result 3, one can show that the optimal parameters are the same as those of the CTPC scheme with $\eta = 1$. Thus, the CTPC scheme is optimal when the power control is perfect, but is sub-optimal otherwise.
- From Result 3, we see that $f_N^*[0] \leq 1/2$, because $0 \leq x \leq 1$, $\epsilon_2(z) > 0$, and $\epsilon_1(z) \leq \epsilon_1(H)$.
- For the CTPC scheme with $\eta = 1$, $\alpha_N[0]$ is one specific solution of a quadratic equation, whose other solution is provably sub-optimal [14]. However, this is no longer the case with imperfect power control. Both solutions of (21) need to be checked for.

Performance Analysis: Unlike the CTPC scheme, the lower target receive power level in the optimal scheme is a function of the interval index i. Now, $\mathcal{S}_{m,n}(i)$ denotes the event that nodes $[1], \ldots, [n]$ target the receive power level H and nodes $[n+1], \ldots, [n+m]$ target the receive power level $L_N[i]$ at time $i\Delta_v$. Let $\mu'_{m,n}(i)$ and $\sigma'_{m,n}(i)$ denote the log-mean and log-deviation, respectively, of the interference plus noise power while decoding the transmission of the best node given $\mathcal{S}_{m,n}(i)$. The optimal success probability can also be obtained from Result 1 except that $\alpha_N[i]$, $\tau_N[i]$, $f_N[i]$, $\varpi_{m,n}$, $\sigma'_{m,n}$, $\mu'_{m,n}$, $g(n,m)$, and $h(n,m)$ are replaced by $\alpha_N^*[i]$, $\tau_N^*[i]$, $f_N^*[i]$, $\varpi_{m,n}(i)$, $\sigma'_{m,n}(i)$, $\mu'_{m,n}(i)$, $e^{\sigma_l^2}\left(e^{\sigma_l^2} - 1\right)\left(nH^2 + m(L_N^*[i])^2\right)$, and $e^{\sigma_l^2/2}\left(nH + mL_N^*[i]\right) + \sigma^2$, respectively. The probability of selecting a non-best node can also be obtained by making similar substitutions in Result 2.

In order to gain insights, we now study the asymptotic regime in which the number of users K is large. We define $\boldsymbol{\beta}_N = \lim_{K\to\infty} K\boldsymbol{\alpha}_N$ and characterize it below. Intuitively, this makes sense because the interval length shrinks as the number of users increases. Otherwise, the probability that a sufficiently large number of nodes transmit and, therefore, the best node cannot be decoded would increase to one.

Result 4: When $K \to \infty$, the optimal success probability is given by

$$P_N^* = \varrho(\beta_N^*[0], f_N^*[0], L_N^*[0]), \tag{22}$$

where $\varrho(x,y,z) = e^{-x}\left(x\,(y\epsilon_1(z) + (1-y)\,\epsilon_1(H)) + x^2 y\,(1-y)\epsilon_2(z) + P_{N-1}^*\right)$. Furthermore, $\beta_N^*[0]$ and $f_N^*[0]$ can be determined in terms of $L_N^*[0]$ as follows:

1) Given $L_N[0] = z$, the scaled interval length $\beta_N[0]$ that maximizes the success probability is equal to $\left(\epsilon_2(z) - \epsilon_1(z) - \epsilon_1(H) + \sqrt{4\epsilon_1(z)\epsilon_1(H) + (\epsilon_2(z))^2 - 4P_{N-1}^*\epsilon_2(z)}\right)/\epsilon_2(z)$.
2) Given $\beta_N[0] = x'$ and $L_N[0] = z$, the fraction $f_N[0]$ that maximizes the success probability is equal to $1/2 - (\epsilon_1(H) - \epsilon_1(z))\,/\,\left(2x'\epsilon_2(z)\right)$.

Furthermore, for $1 \leq i \leq N$,

$$\beta_N^*[i] = \beta_{N-1}^*[i-1],\ f_N^*[i] = f_{N-1}^*[i-1],$$
$$L_N^*[i] = L_{N-1}^*[i-1]. \tag{23}$$

Proof: The proof is given in Appendix E. ■

The above result reduces the number of possibilities to be examined for finding $L_N^*[0]$ by a factor of two compared to Result 3(2). This is because it explicitly gives the optimal scaled interval length $\beta_N[0]$ for a given $L_N[0]$ instead of the two roots that needed to be checked for earlier. More importantly, it also leads to the following perturbation-theoretic result that brings out how the statistics of imperfect power control affect the optimal parameters. For this, we first recall the following result. For the CTPC scheme with $\eta = 1$, the optimal scaled interval length $\beta_N[0]$ and the optimal fraction $f_N[0]$ are given by [14]:

$$\beta_N[0] = -1 + \sqrt{5 - 4P_{N-1}^*} \quad \text{and} \quad f_N[0] = \frac{1}{2}. \tag{24}$$

Corollary 1: Let $\epsilon_1(L_N^*[0]) = 1 - \delta_1$, $\epsilon_1(H) = 1 - \delta_2$, and $\epsilon_2(L_N^*[0]) = 1 - \delta_3$, and $\delta_1, \delta_2, \delta_3 \geq 0$. If δ_1, δ_2, and δ_3 are

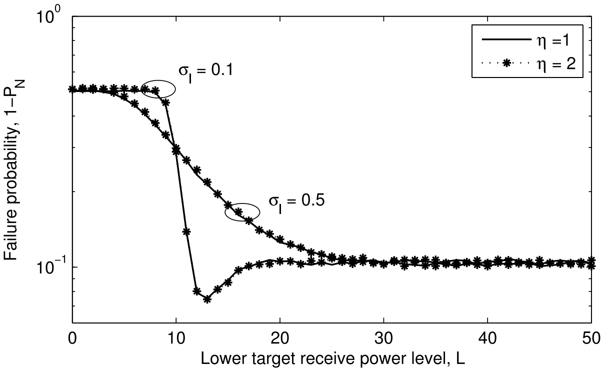

Fig. 2. Failure probability of CTPC scheme as a function of the lower target receive power level L for different values of η and σ_l ($K = 10$, $H = 150$, and $N = 14$).

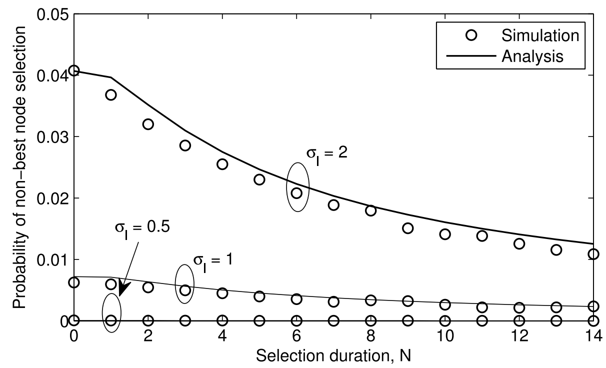

Fig. 3. Zoomed-in view of probability of non-best node selection of the CTPC scheme as a function of N for different σ_l ($\eta = 1$, $K = 10$, $L = 13$, and $H = 150$).

infinitesimally small, then

$$\beta_N^*[0] = -1 + \sqrt{5 - 4P_{N-1}^*} + \psi\left(\delta_1, \delta_2, \delta_3\right), \qquad (25)$$

$$f_N^*[0] = \frac{1}{2} - \frac{\delta_1 - \delta_2}{2\beta_N^*[0]}, \qquad (26)$$

where $\psi\left(\delta_1, \delta_2, \delta_3\right) = \left(\delta_1 + \delta_1\right)\left(1 - 2/\sqrt{5 - 4P_{N-1}^*}\right) + \delta_3\left(\sqrt{5 - 4P_{N-1}^*} - 2 - \left(1 - 2P_{N-1}^*\right)/\sqrt{5 - 4P_{N-1}^*}\right)$.

Proof: The proof is given in Appendix F. ■

Comments: We see that $\psi\left(\delta_1, \delta_2, \delta_3\right)$ in (25) and $\left(\delta_1 - \delta_2\right)/\left(2\beta_N^*[0]\right)$ in (26) are the perturbation terms that arise due to imperfect power control. We also see that $f_N^*[0]$ increases when δ_1 decreases, i.e., when the success probability of the event in which the best node targets the lower receive power level and transmits alone increases.

V. RESULTS

We now evaluate the efficacy of the proposed scheme for different system parameter settings. We verify the analytical results with Monte Carlo simulation results, which are generated using 50 000 runs. In each run, the metrics of the K nodes are generated as independent, uniformly distributed RVs that lie in [0, 1). Their power control errors are generated as independent, lognormal RVs with a log-deviation σ_l. We normalize all the target receive power levels with respect to σ^2, which we set w.l.o.g. to 1, and represent them in linear scale. We set $\gamma = 10$ dB. To ensure better clarity in the figures, we shall often plot the failure probability, which is one minus the success probability. Maximizing the success probability is equivalent to minimizing the failure probability.

A. Performance of Conventional Timer Scheme With Imperfect Power Control

Figure 2 plots the failure probability of the CTPC scheme in logarithmic scale for $\eta = 1$ and 2, and for different values of the lower target receive power level L, in the presence of imperfect power control. We make the following observations. First, increasing η leads to only a marginal decrease in the failure probability. Second, for $L \leq 5$, the failure probability is close to 0.5 because the best node is unlikely to be decoded when it targets such a low L. Third, the behavior of the failure probability as a function of L is different for $\sigma_l = 0.1$ and 0.5. For $\sigma_l = 0.1$ and $\eta = 1$ or 2, the failure probability initially decreases as L increases, attains its lowest value of 0.074 at $L = 13$, and marginally increases again as L increases further. On the other hand, it decreases monotonically for $\sigma_l = 0.5$. However, in both cases, it levels off at 0.1 as L increases. This is because for larger L, the event in which only the best node transmits alone contributes the most to the success probability. Fourth, for $L \leq 9$, the failure probability for $\sigma_l = 0.5$ is less than that for $\sigma_l = 0.1$. This is because the failure probability of the event in which only the best node transmits and targets the receive power level L, which is equal to $1 - Q\left(\ln\left(\gamma\sigma^2/L\right)/\sigma_l\right)$, decreases as σ_l increases. This is the dominant event when any node targets the receive power level L.

Figure 3 plots the probability that a non-best node gets selected as a function of the selection duration N for different σ_l. It increases as σ_l increases. Given σ_l, it decreases as N increases because the probability that multiple nodes transmit simultaneously at any time instant decreases. The marginal gap between the analysis and simulation results arises due to the Fenton-Wilkinson (F-W) method-based approximations [32, Ch. 3] made in Appendix B.

B. Performance and Benchmarking

We now benchmark the performance of the optimal scheme with the widely used IT scheme that uses the mapping $f(\mu) = c/\mu$ to set the timer of a node [8], CT scheme [6], and CTPC scheme with $\eta = 1$ that exploits power control but is designed assuming that it is perfect [14]. In order to maximize the success probabilities of the CT and IT schemes and ensure a fair comparison, we set the target receive power level as H for both of them. Furthermore, we numerically optimize c for each selection duration for the IT scheme.

Figures 4(a) and 4(b) plot the failure probabilities in logarithmic scale of the above mentioned schemes for $\sigma_l = 0.1$ and 0.5, respectively, as a function of N for $K = 10$ and

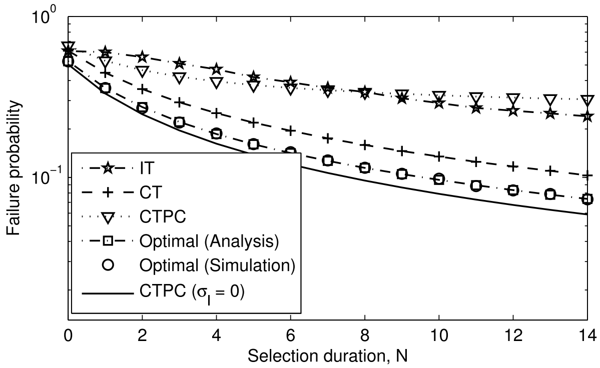

(a) Power control error log-deviation $\sigma_l = 0.1$.

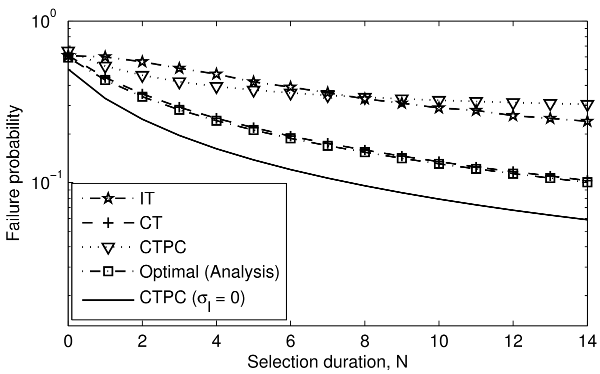

(b) Power control error log-deviation $\sigma_l = 0.5$.

Fig. 4. Performance benchmarking: Failure probability as a function of the selection duration N ($K = 10$ and $H = 150$).

$H = 150$. The metric is a unit mean exponential RV.[4] Also plotted is the failure probability of the CTPC scheme with perfect power control ($\sigma_l = 0$). Figure 4(a) plots both analysis and simulation results for the optimal scheme. We see that there is a good match between the two, which validates the analysis. The same observation holds for Fig. 4(b), in which only analysis results for the optimal scheme are shown in order to avoid clutter.

We observe in Fig. 4(a), in which σ_l is 0.1, that the optimal scheme outperforms the IT, CT, and CTPC schemes. For example, for $N = 14$, the failure probabilities of the optimal, IT, CT, and CTPC schemes are 0.073, 0.24, 0.10, and 0.30, respectively. The performance of the CTPC scheme degrades by 25.0% compared to that with perfect power control. However, for the optimal scheme, this degradation is only 1.1%. In Fig. 4(b), in which σ_l is 0.5, the optimal scheme markedly outperforms IT and CTPC, and marginally outperforms CT. For example, at $N = 14$, the failure probabilities of the optimal, IT, CT, and CTPC schemes are 0.10, 0.24, 0.10, and 0.30, respectively.

These two figures bring out several noteworthy points. First, there is a significant increase in the failure probability of the CTPC scheme due to imperfect power control. This is due to its choice of the lower target receive power level L as $\gamma \sigma^2$ (cf. (2)). When the best node transmits alone and targets the receive power level L, the probability that its SNR falls below γ is now $1 - Q(0) = 1/2$. Secondly, the failure probabilities of the IT and the CT schemes are insensitive to σ_l. This is because of our choice of H as the target receive power level for them. Third, we see that for $\sigma_l = 0.5$, the performance of the CT scheme approaches that of the optimal scheme. This is because the optimal scheme needs to tackle the following two counteracting trends. Increasing $L_N[i]$ increases the probability that the best node gets selected if it happens to transmit alone in i^{th} interval. However, doing so reduces the odds that the best node gets selected if it targets the receive power level H and m other nodes target $L_N[i]$ in the i^{th} interval. For large σ_l, $L_N^*[i]$ turns out to be close to H in order to tackle the first trend, which dominates the success probability. In this regime, the performance of the system is, therefore, just as good as using only one target power level H, which is the case with the CT scheme. However, when σ_l is small, $L_N^*[i]$ is small relative to H and both the trends contribute to the success probability. Here, the optimal scheme does outperform CT, as is seen in Fig. 4(a).

[4]While the performances of the CT, CTPC, and optimal schemes do not depend on the probability distribution of the metric, the performance of the IT scheme does depend on it. Hence, we specify the probability distribution here.

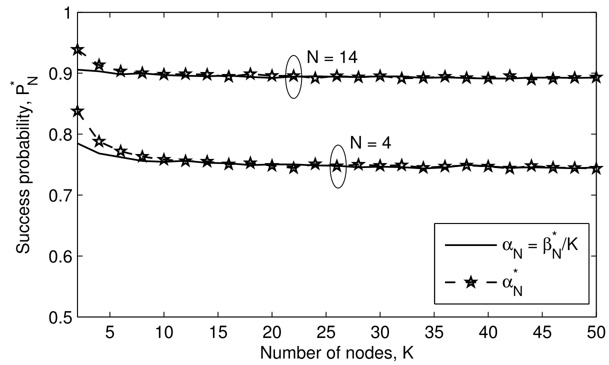

Fig. 5. Asymptotic behavior and scalability: Zoomed-in view of success probability as a function of the number of nodes K for different N and different settings of $\boldsymbol{\alpha}_N$ ($\sigma_l = 0.5$ and $H = 150$).

1) Asymptotics: Figure 5 plots P_N^* as a function of the number of nodes K for two different selection durations. It also plots the success probability of the timer scheme when its ILV, PDV, and LPV are set as $\boldsymbol{\alpha}_N = \boldsymbol{\beta}_N^*/K$, $\boldsymbol{f}_N = \boldsymbol{f}_N^*$, and $\boldsymbol{L}_N = \boldsymbol{L}_N^*$, where $\boldsymbol{\beta}_N^*$, $\boldsymbol{f}_N^*$, and $\boldsymbol{L}_N^*$ are given in Result 4. We observe that the asymptotic regime manifests itself even when K is as small as 10. We also observe that the proposed scheme is scalable even with imperfect power control, since its success probability levels off at 0.89 and 0.74 for $N = 14$ and 4, respectively, and does not decrease to 0 as K increases. This is because the $\alpha_N^*[i]$, which drives how many nodes transmit at time $i\Delta_v$, decreases as K increases.

C. Insights About Structure of Optimal Mapping

Figure 6 plots the interval lengths of the optimal, CT, and CTPC schemes as a function of the interval index i for different values of σ_l for $N = 14$. In all the schemes, the interval length increases with i. This implies that all the schemes are initially conservative and cause fewer nodes,

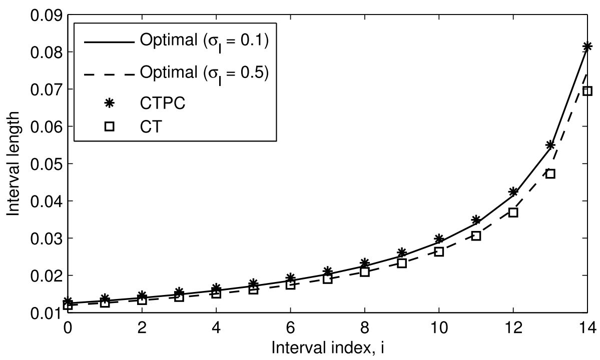

Fig. 6. Effect of power control error log-deviation on optimal interval lengths $\alpha_N^*[i]$ as a function of interval index i ($H = 150$, $N = 14$, and $K = 10$).

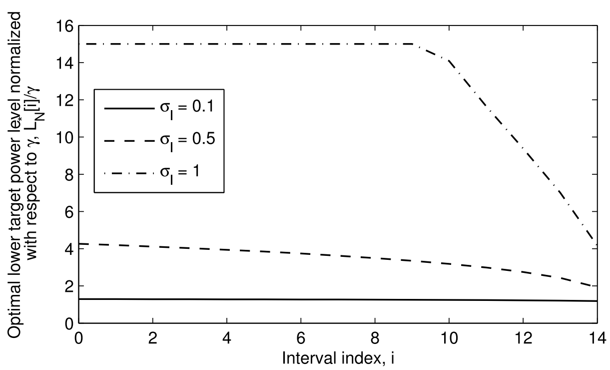

Fig. 7. Optimal lower target receive power level $L_N^*[i]$ normalized with respect to γ as a function of interval index i for different power control error log-deviations ($H = 150$, $N = 14$, and $K = 10$).

on average, to transmit. However, as the time remaining for selection decreases, the lengths of the remaining intervals increase to increase the odds of a transmission.

Figure 7 plots the optimal lower target receive power level $L_N^*[i]$ normalized with respect to γ as a function of the interval index i for different σ_l. We see that for any i, $L_N^*[i]$ increases as σ_l increases. This ensures that the probability that the best node gets selected when it transmits alone and targets $L_N^*[i]$ does not decrease as power control becomes more imperfect. Furthermore, given σ_l, $L_N^*[i]$ decreases as i increases. This is because, as we saw in Fig. 6, the average number of nodes that transmit at time $i\Delta_v$ increases as i increases. Consequently, a decrease in $L_N^*[i]$ increases the selection probability of the best node when it targets H and the other nodes target $L_N^*[i]$ at time $i\Delta_v$. For example, for $\sigma_l = 1$, which corresponds to a relatively large power control error, $L_N^*[i]$ saturates at the highest possible value H for $i \leq 9$ and decreases thereafter.

Figure 8 plots the optimal fraction of nodes $f_N^*[i]$ that target the receive power level $L_N^*[i]$ as a function of the interval index i for different σ_l. For a given i, we see that $f_N^*[i]$ for $\sigma_l = 0.1$ is greater than that for $\sigma_l = 0.5$. This is due to the decrease in $L_N^*[i]$ as σ_l decreases, which we observed in Fig. 7. A lower $L_N^*[i]$ increases the probability that the best node is decoded when it targets H and the interfering nodes target $L_N^*[i]$. A higher $f_N^*[i]$ then facilitates the capture of the best node if it were to target H by increasing the probability that the interfering nodes target $L_N^*[i]$ instead of H.

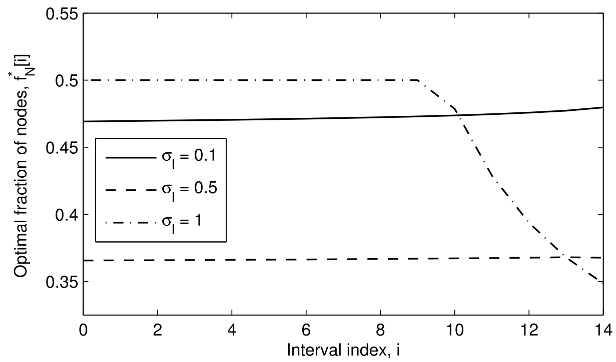

Fig. 8. Zoomed-in view of the optimal fraction of nodes $f_N^*[i]$ that target the receive power level $L_N^*[i]$ as a function of interval index i for different power control error log-deviations ($H = 150$, $N = 14$, and $K = 10$).

We also see that $f_N^*[i]$ increases as i increases for both $\sigma_l = 0.5$ and 0.1. However, the trends for $\sigma_l = 1$ are different. Instead of remaining constant, $f_N^*[i]$ now decreases as i increases. The reason for this is as explained in the previous paragraph.

VI. Conclusions

We analyzed the success probability of the CTPC scheme and saw that it was quite sensitive to the log-deviation of the power control error, which was modeled as a lognormal RV on the basis of the extensive set of results reported in the literature. It also varied over a wide range depending on the choice of its parameters, which were specified in an ad hoc manner. We then developed a new distributed timer scheme, in which the lower target receive power level and the metric-to-timer-and-power mapping were jointly optimized, in order to maximize the success probability given imperfect power control. We presented a recursive computation that significantly reduced the number of variables that had to be jointly optimized, and made a numerical computation of the optimal parameters feasible. Under imperfect power control, the proposed scheme was scalable and achieved a higher success probability than the timer schemes studied in the literature, with the extent of gain depending on the log-deviation of the power control error.

An interesting avenue for future work is to evaluate the system-level trade-offs associated with the use of the timer scheme, with or without power control. These include the power cost and protocol overheads of using power control, feedback overheads, and the spectral efficiency cost of implementing the selection scheme itself. Evaluating the impact of the peak power constraint is another relevant problem.

Appendix

A. Proof of Result 1

The success probability P_N is given by

$$P_N = \sum_{i=0}^{N} \Pr\{\mathcal{S}(i)\}, \tag{27}$$

where $\mathcal{S}(i)$ denotes the success event at time instant $i\Delta_v$.

It occurs if node [1] transmits at time instant $i\Delta_v$ and gets selected. From the law of total probability, we have

$$\Pr\{\mathcal{S}(i)\} = \sum_{m=0}^{K}\sum_{n=0}^{K-m} \varpi_{m,n} \Pr\left\{\mathcal{S}_{m,n}(i)\right\}, \tag{28}$$

where $\varpi_{(m,n)}$ is the probability of success given the event $\mathcal{S}_{m,n}(i)$. Furthermore,

$$\Pr\left\{\mathcal{S}_{m,n}(i)\right\} = \binom{K}{m,n} (\tau_N[i])^{K-(m+n)} (\alpha_N[i])^{m+n} \times (f_N[i])^m (1-f_N[i])^n. \tag{29}$$

We now calculate $\varpi_{m,n}$ for different m and n. When no node transmits, i.e., $m+n=0$, we have $\varpi_{m,n}=0$. When only node [1] transmits, i.e., when $m+n=1$, we have $\mathrm{SINR}_{[1]}(m,n) = q_{[1]}e^{l_{[1]}}/\sigma^2$, where $\mathrm{SINR}_{[j]}(m,n)$ denotes the SINR of node $[j]$ given $\mathcal{S}_{m,n}(i)$. Hence,

$$\varpi_{m,n} = \Pr\left\{\frac{q_{[1]}e^{l_{[1]}}}{\sigma^2} \geq \gamma\right\} = Q\left(\frac{1}{\sigma_l}\ln\left(\frac{\gamma\sigma^2}{q_{[1]}}\right)\right). \tag{30}$$

When multiple nodes transmit simultaneously, i.e., when $m+n \geq 2$, we have

$$\mathrm{SINR}_{[1]}(m,n) = \frac{q_{[1]}e^{l_{[1]}}}{\sum_{k=2}^{m+n} q_{[k]}e^{l_{[k]}} + \sigma^2} \approx \frac{q_{[1]}e^{l_{[1]}}}{e^{l'_{m,n}}}. \tag{31}$$

This follows from the Fenton-Wilkinson method [32, Ch. 3], which approximates $\sum_{k=2}^{m+n} q_{[k]}e^{l_{[k]}} + \sigma^2$ by a lognormal RV $e^{l'_{m,n}}$, where $l' \sim \mathcal{N}\left(\mu'_{m,n}, \sigma'^2_{m,n}\right)$. The values of $\sigma'^2_{m,n}$ and $\mu'_{m,n}$ for different m and n are given in (9) and (10), respectively. Hence, we get $\varpi(m,n) \approx \Pr\left\{q_{[1]}e^{l_{[1]}}/e^{l'_{m,n}} \geq \gamma\right\}$, which simplifies to (8).

B. Proof of Result 2

From assumption (ii) in Section III, the probability that node $[j]$ is selected is zero for $j \geq 3$. Therefore, the probability P_N^{other} that a non-best node is selected is

$$\begin{aligned} P_N^{\text{other}} &= \Pr\{\text{Node [2] selected}\}, \\ &= \sum_{i=0}^{N}\sum_{m=0}^{K}\sum_{n=0}^{K-m} \Pr\left\{\mathcal{S}_{m,n}(i)\right\} \varpi'_{(m,n)}, \end{aligned} \tag{32}$$

where $\varpi'_{(m,n)} = \Pr\left\{\mathrm{SINR}_{[2]}(m,n) \geq \gamma\right\}$ is the probability that node [2] is selected given $\mathcal{S}_{m,n}(i)$.

When $m+n \leq 1$, node [2] does not transmit. Hence, $\varpi'_{(m,n)} = 0$. When multiple nodes transmit at time $t = i\Delta_v$, the SINR of node [2] is

$$\mathrm{SINR}_{[2]}(m,n) = \frac{q_{[2]}e^{l_{[2]}}}{\sum_{k=1,k\neq 2}^{m+n} q_{[k]}e^{l_{[k]}} + \sigma^2} \approx \frac{q_{[2]}e^{l_{[2]}}}{e^{l''_{m,n}}}. \tag{33}$$

As before, $\sum_{k=1,k\neq 2}^{m+n} q_{[k]}e^{l_{[k]}} + \sigma^2$ is approximated using the F-W method by a lognormal RV $e^{l''_{m,n}}$, where $l''_{m,n} \sim \mathcal{N}\left(\mu''_{m,n}, \sigma''^2_{m,n}\right)$. The values of $\sigma''^2_{m,n}$ and $\mu''_{m,n}$ for different m and different n are given in (13) and (14), respectively. Hence, for $m+n \geq 2$, $\varpi'_{(m,n)}$ is as given in (12).

C. Computation of $Pr\{S_0(x,y,z)\}$

From the law of total probability, the probability of success at $t=0$ is given by

$$\begin{aligned} &\Pr\{S_0(\alpha_N[0], f_N[0]), L_N[0])\} \\ &= \sum_{m=0}^{K}\sum_{n=0}^{K-m} \Pr\left\{\mathcal{S}_{m,n}(0)\right\} \Pr\left\{\text{Success}|\mathcal{S}_{m,n}(0)\right\}, \end{aligned} \tag{34}$$

where $\mathcal{S}_{m,n}(i)$ denotes the event in which nodes $[1],\ldots,[n]$ target the receive power level H and nodes $[n+1],\ldots,[n+m]$ target $L_N[i]$ at time $i\Delta_v$. Given $\mathcal{S}_{m,n}(0)$, we have $\mathrm{SINR}_{[1]}(m,n) = q_{[1]}e^{l_{[1]}}/\left(\sum_{k=2}^{m+n} q_{[k]}e^{l_{[k]}} + \sigma^2\right)$, where $q_{[k]} \in \{L_N[0], H\}$, for $1 \leq k \leq m+n$. Thus,

$$\Pr\left\{\text{Success}|\mathcal{S}_{m,n}(0)\right\} = \Pr\left\{\frac{q_{[1]}e^{l_{[1]}}}{\sum_{k=2}^{m+n} q_{[k]}e^{l_{[k]}} + \sigma^2} \geq \gamma\right\}. \tag{35}$$

A success occurs at time $t=0$ if: (i) Only node [1] transmits at $t=0$ and it targets receive power level H, which occurs with probability $K\alpha_N[0](1-\alpha_N[0])^{K-1}(1-f_N[0])$, and $\mathrm{SINR}_{[1]} = He^{l_{[1]}}/\sigma^2 \geq \gamma$. The probability that $\mathrm{SINR}_{[1]}$ exceeds γ is $\epsilon_1(H) = Q\left(\ln\left(\sigma^2\gamma/H\right)/\sigma_l\right)$. Hence, the probability of this event is $K\alpha_N[0](1-\alpha_N[0])^{K-1}(1-f_N[0])\epsilon_1(H)$. Or, (ii) Only node [1] transmits at $t=0$ and it targets receive power level $L_N[0]$, and $\mathrm{SINR}_{[1]} = L_N[0]e^{l_{[1]}}/\sigma^2 \geq \gamma$. The probability of this event is $K\alpha_N[0](1-\alpha_N[0])^{K-1}f_N[0]\epsilon_1(L_N[0])$. Or, (iii) Only nodes [1] and [2] transmit at $t=0$ and they target H and $L_N[0]$, respectively, which occurs with probability $\binom{K}{1,1}(\alpha_N[0])^2(1-\alpha_N[0])^{k-2}(1-f_N[0])f_N[0]$, and $\mathrm{SINR}_{[1]} \geq \gamma$. Here,

$$\mathrm{SINR}_{[1]} = \frac{He^{l_{[1]}}}{L_N[0]e^{l_{[2]}} + \sigma^2} \approx \frac{He^{l_{[1]}}}{e^{\grave{l}}}, \tag{36}$$

where $e^{\grave{l}}$ is the lognormal approximation of $L_N[0]e^{l_{[2]}} + \sigma^2$ using the F-W method and $\grave{l} \sim \mathcal{N}(\grave{\mu}, \grave{\sigma}^2)$. The values of $\grave{\mu}$ and $\grave{\sigma}^2$ for $L_N[0] = z$ are given below (18). Hence, the probability of this event is $\binom{K}{1,1}(\alpha_N[0])^2(1-\alpha_N[0])^{k-2}(1-f_N[0])f_N[0]\epsilon_2(L_N[0])$.

We neglect the negligible contributions from the following remaining events: a) three or more nodes transmit simultaneously, and b) nodes [1] and [2] target same receive power level and a success occurs. Summing the above three probabilities yields (18).

D. Proof of Result 3

We first state the following two intermediate results before computing the optimal parameters:

1) $\alpha_N^*[0] \in (0,1)$: We prove this by showing that $\alpha_N^*[0] = 0$ or 1 is sub-optimal.

a) Proof that $\alpha_N^*[0] = 0$ is Sub-optimal: Let

$$U_N(x,y,z) = \Pr\{S_0(x,y,z)\} + (1-x)^K P_{N-1}^*. \tag{37}$$

Recall from Section IV that $\Pr\{S_0(x,y,z)\} = Kx(1-x)^{K-1}(y\epsilon_1(z) + (1-y)\epsilon_1(H)) + \binom{K}{1,1}x^2(1-x)^{K-2}(1-y)y\epsilon_2(z)$. From (16), (18), and the fact that $P_{N-1}^* \geq P_{N-1}(\boldsymbol{\alpha}_{N-1}, \boldsymbol{f}_{N-1}, \boldsymbol{L}_{N-1})$, for any ILV $\boldsymbol{\alpha}_{N-1}$, PDV $\boldsymbol{f}_{N-1}$, and LPV $\boldsymbol{L}_{N-1}$, we see that $U_N(x, y, z)$ is the maximum success probability given $\alpha_N[0] = x$, $f_N[0] = y$, and $L_N[0] = z$. When $\alpha_N^*[0] = 0$, we see from (20) that $P_N^* = P_{N-1}^*$. Now, consider the parameters $\alpha_N[0] = \delta$, where $0 < \delta \ll 1$, $f_N[0] = 1/2$, and $L_N[0] = H$. For these parameters, we get

$$U_N\left(\delta, \frac{1}{2}, H\right) = K\delta(\epsilon_1(H) - P_{N-1}^*) + P_{N-1}^* + O\left(\delta^2\right) > P_{N-1}^* = P_N^*. \quad (38)$$

This is because $P_{N-1}^* < \epsilon_1(H)$ since $\epsilon_1(H)$ is the same as the success probability of a genie-aided scheme that always makes the best node transmit alone with H. Hence, $\alpha_N^*[0] = 0$ is sub-optimal.

b) Proof that $\alpha_N^*[0] = 1$ is Sub-optimal: Consider first the case where $K \geq 3$. From (20), it follows that $P_N^* = 0$ for $\alpha_N^*[0] = 1$. It is obvious from (37) that $U_N(1-\delta, 1/2, H/2)$, where $0 < \delta < 1$, is greater than P_N^*. Hence, $\alpha_N^*[0] = 1$ is sub-optimal.

The only other case is $K = 2$. When $\alpha_N^*[0] = 1$, we have $P_N^* = 2(1 - f_N^*[0]) f_N^*[0] \epsilon_2(L_N^*[0])$, which is maximized when $f_N^*[0] = 1/2$. Hence, $P_N^* = \epsilon_2(L_N^*[0])/2$. Now, consider the success probability for the parameters $\alpha_N[0] = 1 - \delta$, where $0 < \delta \ll 1$, $f_N[0] = 1/2$, and $L_N[0] = L_N^*[0]$:

$$\begin{aligned} &U_N\left(1-\delta, \frac{1}{2}, L_N^*[0]\right) \\ &= 2\delta\left(\frac{\epsilon_1(L_N^*[0])}{2} + \frac{\epsilon_1(H)}{2}\right) + \frac{(2-4\delta)\epsilon_2(L_N^*[0])}{4} + O(\delta^2), \\ &= \delta(\epsilon_1(L_N^*[0]) + \epsilon_1(H) - \epsilon_2(L_N^*[0])) + P_N^* + O(\delta^2). \end{aligned} \quad (39)$$

By definition of $\epsilon_1(\cdot)$, we know that $\epsilon_1(H) \geq \epsilon_2(L_N^*[0])$. Hence, $U_N(1-\delta, 1/2, L_N^*[0]) > P_N^*$. Hence, $\alpha_N^*[0] = 1$ is sub-optimal for all $K \geq 2$.

2) $f_N^*[0] \in (0, 1)$: Its proof is similar to that above, and is skipped to conserve space.

The second result above implies that the derivative $\partial U_N\left(\alpha_N^*[0], y, L_N^*[0]\right)/\partial y$ must be equal to 0 at $y = f_N^*[0]$. The partial derivative of the success probability $U_N(x, y, z)$ with respect to y equals

$$\frac{\partial U_N(x, y, z)}{\partial y} = Kx(1-x)^{K-2}\left((1-x)(\epsilon_1(z) - \epsilon_1(H)) + (K-1)x(1-2y)\epsilon_2(z)\right). \quad (40)$$

Equating it to zero yields $y = 1/2 - (1-x)\left(\epsilon_1(H) - \epsilon_1(z)\right) / (2(K-1)x\epsilon_2(z))$, which is Result 3(1). For this value of y, let $h_N(x, z) = U_N(x, 1/2 - (1-x)(\epsilon_1(H) - \epsilon_1(z)) / (2x(K-1)\epsilon_2(z)), z)$. The first result above implies that $\partial h_N(x, L_N^*[0])/\partial x = 0$ at $x = \alpha_N^*[0]$. The partial derivative of $h_N(x, z)$ with respect to x is given by

$$\begin{aligned} \frac{\partial h_N(x, z)}{\partial x} &= \left[\frac{K(1-x)^2\chi_3(z)}{4\chi_2(z)} - \frac{Kx^2}{4} + \frac{x}{2}\right] \\ &\quad \times 2K\chi_2(z)(1-x)^{K-3} \\ &\quad + \left[(1-Kx)\chi_1(z) - K(1-x)\chi_3(z)\right] \\ &\quad \times K(1-x)^{K-2} - K(1-x)^{K-1}P_{N-1}^*. \end{aligned} \quad (41)$$

Equating it to zero yields the quadratic equation in (21).

E. Proof of Result 4

In (21), when $K \to \infty$, we have $a(z)/K^2 \to -\epsilon_2(z)/4$, $b(z)/K \to \epsilon_2(z)/2 - \chi_1(z)$, and $c(z) \to \chi_1(z) - (\epsilon_1(z) - \epsilon_1(H))^2/(4\epsilon_2(z)) - P_{N-1}^*$. For a given $L_N[0] = z$, the optimal interval length is one of the two solutions of (21), which we denote by $\rho_{a1}(z)$ and $\rho_{a2}(z)$. When $K \to \infty$, we have

$$\lim_{K\to\infty} K\rho_{a1}(z) = \xi_1(z) + \xi_2(z), \quad (42a)$$

$$\lim_{K\to\infty} K\rho_{a2}(z) = \xi_1(z) - \xi_2(z), \quad (42b)$$

where $\xi_1(z) = (\epsilon_2(z) - \epsilon_1(z) - \epsilon_1(H))/\epsilon_2(z)$ and $\xi_2(z) = \sqrt{4\epsilon_1(z)\epsilon_1(H) + (\epsilon_2(z))^2 - 4P_{N-1}^*\epsilon_2(z)}/\epsilon_2(z)$. We see that $\xi_1(z) < 0$ because $\epsilon_1(H) > \epsilon_2(z)$. This implies that $\lim_{K\to\infty} K\rho_{a2}(z) < 0$. Hence, for a given $L_N[0] = z$, the optimal scaled interval length is $\xi_1(z) + \xi_2(z)$, which yields Result 4(1). This also shows that $\alpha_N^*[0] \to 0$ as $K \to \infty$.

Result 4(2) directly follows from Result 3(1). From (16), (17), and (20), we see that $\alpha_N^*[i] = \alpha_{N-1}^*[i-1](1 - \alpha_N^*[0])$, $f_N^*[i] = f_{N-1}^*[i-1]$, and $L_N^*[i] = L_{N-1}^*[i-1]$, for $1 \leq i \leq N$. This and the fact that $\alpha_N^*[0] \to 0$ as $K \to \infty$ directly lead to the recursions for the remaining elements of $\boldsymbol{\beta}_N^*$, $\boldsymbol{f}_N^*$, and $\boldsymbol{L}_N^*$ that are given in (23). Lastly, we evaluate the success probability P_N^*. Since $\beta_N^*[0] = \lim_{K\to\infty} K\alpha_N^*[0]$, substituting $\lim_{K\to\infty} (1 - \alpha_N^*[0])^K = \lim_{K\to\infty}\left(1 - \beta_N^*[0]/K\right)^K = e^{-\beta_N^*[0]}$ in (20) yields (22).

F. Proof of Corollary 1

Substituting $\epsilon_1(L_N^*[0]) = 1 - \delta_1$, $\epsilon_1(H) = 1 - \delta_2$, and $\epsilon_2(L_N^*[0]) = 1 - \delta_3$ in the expression for $\beta_N^*[0] = \lim_{K\to\infty} K\rho_{a1}(L_N^*[0])$ in (42a), and using the fact that δ_1, δ_2, $\delta_3 \ll 1$, we get

$$\begin{aligned} \beta_N^*[0] &\approx (1-\delta_3)^{-1}\Big(-1 + \delta_1 + \delta_2 - \delta_3 \\ &\quad + \sqrt{4(1-\delta_1-\delta_2) + 1 - 2\delta_3 - 4P_{N-1}^*(1-\delta_3)}\Big), \\ &= (1-\delta_3)^{-1}\Big(-1 + \delta_1 + \delta_2 - \delta_3 \\ &\quad + \sqrt{5 - 4P_{N-1}^*}\sqrt{1 - \frac{4\delta_1 + 4\delta_2 + 2\delta_3 - 4P_{N-1}^*\delta_3}{5 - 4P_{N-1}^*}}\Big). \end{aligned}$$

Using the binomial approximations $(1-\delta_3)^{-1} \approx 1 + \delta_3$ and $\left(1 - \left(4\delta_1 + 4\delta_2 + 2\delta_3 - 4P_{N-1}^*\delta_3\right) / \left(5 - 4P_{N-1}^*\right)\right)^{1/2} \approx 1 - \left(2\delta_1 + 2\delta_2 + \delta_3 - 2P_{N-1}^*\delta_3\right) / \left(5 - 4P_{N-1}^*\right)$, we get

$$\begin{aligned} \beta_N^*[0] &\approx (1+\delta_3)\Big(-1 + \delta_1 + \delta_2 - \delta_3 \\ &\quad + \sqrt{5 - 4P_{N-1}^*}\left[1 - \frac{2\delta_1 + 2\delta_2 + \delta_3 - 2P_{N-1}^*\delta_3}{5 - 4P_{N-1}^*}\right]\Big), \\ &\approx -1 + \sqrt{5 - 4P_{N-1}^*} + \psi(\delta_1, \delta_2, \delta_3), \end{aligned}$$

where $\psi(\delta_1, \delta_2, \delta_3)$ is defined in Corollary 1. Lastly, the expression for $f_N^*[0]$ in (26) follows by substituting $z = L_N^*[0]$ and $x' = \beta_N^*[0]$, and using $(1-\delta_3)^{-1} \approx 1 + \delta_3$ in Result 4(2).

REFERENCES

[1] A. S. Ibrahim, A. K. Sadek, W. Su, and K. J. R. Liu, "Cooperative communications with relay-selection: When to cooperate and whom to cooperate with?" *IEEE Trans. Wireless Commun.*, vol. 7, no. 7, pp. 2814–2827, Jul. 2008.

[2] Y. Zhao, R. Adve, and T. J. Lim, "Improving amplify-and-forward relay networks: Optimal power allocation versus selection," *IEEE Trans. Wireless Commun.*, vol. 6, no. 8, pp. 3114–3123, Aug. 2007.

[3] A. J. Goldsmith, *Wireless Communications*, 1st ed. Cambridge, U.K.: Cambridge Univ. Press, 2005.

[4] Y. Chen and Q. Zhao, "An integrated approach to energy-aware medium access for wireless sensor networks," *IEEE Trans. Signal Process.*, vol. 55, no. 7, pp. 3429–3444, Jul. 2007.

[5] A. Attar, N. Devroye, H. Li, and V. C. M. Leung, "A unified scheduling framework based on virtual timers for selfish-policy shared spectrum," in *Proc. ICC*, May 2010, pp. 1–5.

[6] V. Shah, N. B. Mehta, and R. Yim, "Optimal timer based selection schemes," *IEEE Trans. Commun.*, vol. 58, no. 6, pp. 1814–1823, Jun. 2010.

[7] R. Talak and N. B. Mehta, "Optimal timer-based best node selection for wireless systems with unknown number of nodes," *IEEE Trans. Commun.*, vol. 61, no. 11, pp. 4475–4485, Nov. 2013.

[8] A. Bletsas, A. Khisti, D. P. Reed, and A. Lippman, "A simple cooperative diversity method based on network path selection," *IEEE J. Sel. Areas Commun.*, vol. 24, no. 3, pp. 659–672, Mar. 2006.

[9] Q. Zhao and L. Tong, "Opportunistic carrier sensing for energy-efficient information retrieval in sensor networks," *EURASIP J. Wireless Commun. Netw.*, vol. 2005, no. 2, pp. 231–241, Apr. 2005.

[10] Y. Xiao and L. J. Cimini, "Impact of overhead on spectral efficiency of cooperative relaying," *IEEE Trans. Wireless Commun.*, vol. 12, no. 5, pp. 2228–2239, May 2013.

[11] L. Kleinrock and F. Tobagi, "Packet switching in radio channels: Part I—Carrier sense multiple-access modes and their throughput-delay characteristics," *IEEE Trans. Commun.*, vol. COM-23, no. 4, pp. 1400–1416, Dec. 1975.

[12] D. Bertsekas and R. Gallager, *Data Networks*, 2nd ed. Englewood Cliffs, NJ, USA: Prentice-Hall, 1992.

[13] *Part 11: Wireless LAN Medium Access Control (MAC) and Physical Layer (PHY) Specifications*, IEEE Standard 802.11-2007, IEEE Computer Society, Jun. 2007.

[14] V. K. Dewangan and N. B. Mehta, "Timer-based distributed node selection scheme exploiting power control and capture," *IEEE Trans. Wireless Commun.*, vol. 14, no. 3, pp. 1457–1467, Mar. 2015.

[15] A. Zanella and M. Zorzi, "Theoretical analysis of the capture probability in wireless systems with multiple packet reception capabilities," *IEEE Trans. Commun.*, vol. 60, no. 4, pp. 1058–1071, Apr. 2012.

[16] R. Yim, N. B. Mehta, and A. F. Molisch, "Fast Multiple Access Selection through variable power transmissions," *IEEE Trans. Wireless Commun.*, vol. 8, no. 4, pp. 1962–1973, Apr. 2009.

[17] A. Kumar, D. Manjunath, and J. Kuri, *Communication Networking*. San Mateo, CA, USA: Morgan Kaufmann, 2004.

[18] M. G. Jansen and R. Prasad, "Capacity, throughput, and delay analysis of a cellular DS CDMA system with imperfect power control and imperfect sectorization," *IEEE Trans. Veh. Technol.*, vol. 44, no. 1, pp. 67–75, Feb. 1995.

[19] G. E. Corazza, G. De Maio, and F. Vatalaro, "CDMA cellular systems performance with fading, shadowing, and imperfect power control," *IEEE Trans. Veh. Technol.*, vol. 47, no. 2, pp. 450–459, May 1998.

[20] V. Mpako and F. Takawira, "Effects of power control error on the performance of spread ALOHA protocols," in *Proc. COMSIG*, Sep. 1998, pp. 149–154.

[21] V. K. Dewangan and N. B. Mehta, "Capture-induced, fast, distributed, splitting based selection with imperfect power control," *IEEE Trans. Commun.*, vol. 62, no. 1, pp. 74–84, Jan. 2014.

[22] X. Qin and R. Berry, "Exploiting multiuser diversity for medium access control in wireless networks," in *Proc. INFOCOM*, Apr. 2003, pp. 1084–1094.

[23] T. Tang and R. W. Heath, "Opportunistic feedback for downlink multiuser diversity," *IEEE Commun. Lett.*, vol. 9, no. 10, pp. 948–950, Oct. 2005.

[24] C. S. Hwang and J. M. Cioffi, "Opportunistic CSMA/CA for achieving multi-user diversity in wireless LAN," *IEEE Trans. Wireless Commun.*, vol. 8, no. 6, pp. 2972–2982, Jun. 2009.

[25] A. Papoulis and S. U. Pillai, *Probability, Random Variables and Stochastic Processes*, 4th ed. New York, NY, USA: McGraw-Hill, 2002.

[26] A. J. Izenman, "Recent developments in nonparametric density estimation," *J. Amer. Stat. Assoc.*, vol. 86, no. 413, pp. 205–224, Mar. 1991.

[27] A. J. Goldsmith, L. J. Greenstein, and G. J. Foschini, "Error statistics of real-time power measurements in cellular channels with multipath and shadowing," *IEEE Trans. Veh. Technol.*, vol. 43, no. 3, pp. 439–446, Aug. 1994.

[28] A. M. Monk and L. B. Milstein, "Open-loop power control error in a land mobile satellite system," *IEEE J. Sel. Areas Commun.*, vol. 13, no. 2, pp. 205–212, Feb. 1995.

[29] A. J. Viterbi, A. M. Viterbi, and E. Zehavi, "Performance of power-controlled wideband terrestrial digital communication," *IEEE Trans. Wireless Commun.*, vol. 41, no. 4, pp. 559–569, Apr. 1993.

[30] A. J. Viterbi and R. Padovani, "Implications of mobile cellular CDMA," *IEEE Commun. Mag.*, vol. 30, no. 12, pp. 38–41, Dec. 1992.

[31] H.-J. Su and E. Geraniotis, "Adaptive closed-loop power control with quantized feedback and loop filtering," *IEEE Trans. Wireless Commun.*, vol. 1, no. 1, pp. 76–86, Jan. 2002.

[32] G. L. Stüber, *Principles of Mobile Communication*, 2nd ed. Norwell, MA, USA: Kluwer, 2001.

Vikas Kumar Dewangan received the B.E. degree in electronics and communication engineering from the Maulana Azad College of Technology, Bhopal, India, in 1998, the M.Tech. degree in communication and radar engineering from IIT Delhi, New Delhi, India, in 1999, and the Ph.D. degree from the Indian Institute of Science, Bengaluru, India, in 2015. He is a Scientist with the Defence Research and Development Organization, India. His research interest includes multiple access protocols, radar data and signal processing, and target identification.

Neelesh B. Mehta (S'98–M'01–SM'06) received the B.Tech. degree in electronics and communications engineering from IIT Madras, Chennai, India, in 1996, and the M.S. and Ph.D. degrees in electrical engineering from the California Institute of Technology, Pasadena, CA, USA, in 1997 and 2001, respectively. He is a Professor with the Department of Electrical Communication Engineering, Indian Institute of Science, Bengaluru, India. He is a fellow of the Indian National Academy of Engineering and the National Academy of Sciences India. He served on the Board of Governors of the IEEE ComSoc from 2012 to 2015. He serves as the Chair of the Executive Editorial Committee of the IEEE TRANSACTIONS ON WIRELESS COMMUNICATIONS. He also serves as an Editor for the IEEE TRANSACTIONS ON COMMUNICATIONS.